Published in final edited form as:
Proteins. 2014 October ; 82(10): 2874–2878. doi:10.1002/prot.24616.

Crystal structure of the C-terminal domain of mouse TLR9

Bernard Collins[1] and **Ian A. Wilson**[1,2,*]

[1]Department of Integrative Structural and Computational Biology, The Scripps Research Institute, La Jolla, California, USA

[2]Skaggs Institute for Chemical Biology, The Scripps Research Institute, La Jolla, California, USA

Abstract

Toll-like receptors (TLRs) are important pattern recognition receptors that function in innate immunity. Elucidating the structure and signaling mechanisms of TLR9, a sensor of foreign and endogenous DNA, is essential for understanding its critical roles in immunity and autoimmunity. Abundant evidence suggests that the TLR9-CTD (C-terminal domain) by itself is capable of DNA-binding and signaling. We present the crystal structure of unliganded mouse TLR9-CTD. TLR9-CTD exhibits one unique feature, a cluster of stacked aromatic and arginine side chains on its concave face. Overall, its structure is most related to the TLR8-CTD, suggesting a similar mode of ligand binding and signaling.

Keywords

Innate immunity; Toll-like receptor; TLR; TLR9; DNA; nucleic acid; leucine rich repeat; LRR

Introduction

Toll-like receptors (TLRs) comprise an important family of pattern recognition receptors. They play central roles in the innate immune system, link innate immunity to adaptive immunity, and are critical for effective host defenses against numerous pathogens[1]. TLRs can also play detrimental roles in some contexts, such as in septic shock[2] and autoimmunity[3].

Nucleic acid-sensing TLRs, such as TLR3 and TLR7-9, are of particular interest, as they are important for detecting the presence of nucleic acids derived from pathogenic viruses and bacteria and initiate the production of essential pro-inflammatory cytokines and type I interferons[1,4]. TLR7 and TLR9 have also been strongly implicated in contributing to autoimmunity[3].

*Correspondence to: Ian A. Wilson, Department of Integrative Structural and Computational Biology, BCC206, 10550 N. Torrey Pines Rd., La Jolla, California 92037, USA. Tel.: 1-858-784-9706; Fax: 1-858-784-2980; wilson@scripps.edu.

Accession Numbers

The structure factors and atomic coordinates of mTLR9-cECD will be deposited in the RCSB Protein Data Bank (http://www.rcsb.org/) prior to publication with PDB code 4QDH.

The authors declare no competing financial interests.

TLRs are single-pass type I integral membrane proteins with an extracellular ligand-binding domain, a transmembrane domain, and an intracellular signaling (TIR) domain[5]. The ligand binding domain is comprised of several leucine-rich repeats (LRRs) (containing 24 residues per LRR on average), which stack adjacent to each other, forming a large horseshoe-shaped solenoid structure. The concave surface is comprised of a parallel β-sheet, while the convex surface is a mixture of α-helices and unstructured loops. These two surfaces are connected by ascending and descending lateral faces.

The ligand binding and signaling mechanisms of some TLRs have been elucidated. Ligands bind directly (except in the case of TLR4) to the ascending lateral face of TLR dimers[5,8]. Dimerization and/or ligand-induced conformational changes to pre-formed dimers bring the two C-termini into proximity, which presumably then juxtaposes their intracellular TIR domains, thereby initiating signal transduction via dimeric TIR domain-containing adaptors.

TLR9 is a member of the sub-family of TLRs that sense nucleic acids. Like the other members of this group (TLR3, 7, 8), TLR9 is expressed in the ER and traffics to endosomes[6]. These TLRs, including TLR9, also contain a long insertion (coined the "Z-loop" [7]) (Fig. 1A) between two of the central LRRs (LRR14 and 15), approximately in the middle of the ectodomain. Initially, it was thought that cleavage of this loop by resident (endosomal) proteases generated an active receptor comprised of only the C-terminal domain. The C-terminal fragment of TLR9 is competent to bind DNA from microbes that traffic to endosomal compartments and activate downstream pathways[8]. However, this view of signaling by endosomal TLRs has become somewhat controversial[9]. Compared to the full-length TLR9 ectodomain, the CTD binds to DNA with lower affinity, and activation via the CTD leads to reduced signaling and cytokine production[8]. Additionally, recent evidence suggests that the N-terminus of TLR9 is also important for ligand binding and signaling[10,11] and that the two halves remain associated after cleavage of the Z-loop[10] (as observed in the TLR8 structure[7]).

Although the structures, ligand binding modes, and signaling mechanisms of other TLRs have been elucidated, very few of these important characteristics have been uncovered for the nucleic acid-binding TLRs. Our current understanding on these TLRs comes from structural studies of TLR3[12,13] and TLR8[7] (bound to dsRNA and Resiquimod, respectively) that suggest that nucleic acid-binding TLRs follow the same general ligand-binding and activation paradigm as other TLRs: in the active conformation, the ligand is bound (directly) to both ascending lateral faces of the TLR dimer, with the C-termini positioned in close proximity to one another. Interestingly, the N-termini of both receptors make direct contacts with the ligand. To date, no structures of TLR9 or TLR8 are available with a natural ligand.

Because of the key roles of nucleic acid-sensing TLRs in immunity and autoimmunity, the development of signaling modulators (as vaccine adjuvants or therapeutics) is of great importance. In fact, some nucleic acids and nucleic acid analogues targeting these TLRs have proven effective in several clinical scenarios and many more are under development[14]. However, the structural and mechanistic details of TLR7-9 activation remain obscure. In an effort to investigate these issues that should aid in the design of signaling modulators, we have determined the crystal structure of mouse TLR9-CTD.

Materials and Methods

Protein production and crystallization

C-terminally His-tagged mouse TLR9-CTD (residues 480-752) (UniProtID Q9EQU3) with N- and C-terminal hagfish variable lymphocyte receptor (VLR) caps (UniProtID Q4G1L2) (residues 21-81 and 125-200, respectively) was cloned into pFastBac1 (Life Technologies, Inc.) with a gp67 signal sequence. Protein was expressed in Hi5 cells infected with high-titer virus for 3 days at 19C. Cultures were centrifuged and TLR9-CTD was purified from the supernatant using affinity (Ni-NTA) and size-exclusion chromatography (in 25mM HEPES pH 7.5, 150mM NaCl) (16/60 Superdex S200 prep grade, Amersham). The His6-tag was not removed from the protein. Pooled size-exclusion fractions were concentrated to 2.3mg/mL. Crystals were grown by the vapor diffusion method in 1+1 uL sitting drops in 100mM sodium citrate pH 4.77 and 1.5M ammonium sulfate.

Data collection, structure solution, and refinement

Crystals were harvested and flash-cooled in liquid nitrogen without added cryoprotectant. Crystals were screened and data were collected at the ID23 beamline at the Advanced Photon Source (APS). Data from a crystal that diffracted to 2.4 Å were processed with XDS[15]. Data collection statistics are tabulated in Table I. The structure was determined by molecular replacement with Phenix[16] (www.phenix-online.org) using VLR cap structures [PDBID 2Z66[17] and 2Z7X[18]] and a homology model based on the equivalent fragment of TLR8 [PDBID 3W3G[7]]). Model building was performed using Coot[19] (www2.mrc-lmb.cam.ac.uk/personal/pemsley/coot/) and the structure was refined using Phenix. Glycan geometry was monitored with the PDB CArbohydrate REsidue check **(**PDBCARE) online tool (www.glycosciences.de).

Results and Discussion

Protein Expression & Crystallization

Several constructs of TLR9-CTD were tested for expression in the baculovirus expression system, including TLR-variable lymphocyte receptor (VLR) hybrids, a method that has proven successful for determining the structures of other TLR proteins[20]. The TLR9-CTD construct containing VLR caps on both N- and C-termini (Fig. 1A) was expressed at reasonable (approximately 300ug per liter of culture), predominantly as a monomer (Fig. S1A), and crystallized in several conditions.

The asymmetric unit of TLR9-CTD crystals contained a dimer in an anti-parallel configuration (Fig. 1B). Interestingly, the ascending lateral faces (likely ligand binding sites) of each monomer are facing one another, as would be expected in the activated form of the receptor. However, the anti-parallel orientation suggests that this dimer is not physiologically relevant. The C-termini of TLRs are always positioned proximal to the plasma membrane; therefore biologically relevant dimers always exist in a parallel orientation.

Although many attempts were made to obtain a TLR9-CTD:DNA complex, none were successful thus far. Multiple CTD constructs were used in co-crystallization and crystal-

soaking experiments with a variety of DNA oligomers and nucleotides. However, although diffraction-quality crystals were obtained in many of these co-crystallization experiments, no density was observed for any of these ligands.

Structure of TLR9-CTD

As expected, the overall structure of TLR9-CTD is similar to other TLRs. The LRRs form a curved solenoid-like structure with a concave face comprised of a parallel β-sheet and a convex face with variable features, including loops and α-helices (Fig. 1C). The ascending lateral face of the CTD, which is the putative DNA-binding interface, is glycan-free.

The TLR9-CTD structure exhibits similarities to the structures of other nucleic acid-binding TLRs, particularly TLR8. Similar to TLR3[12] and TLR8[7], the electrostatic surface potentials are comprised of a mixture of positively and negatively charged regions (Fig. S1B); thus, no obvious potential nucleic acid binding sites can be easily inferred. Additionally, similar to the TLR8 and hTLR3 structures, several ordered SO4 ions were observed in the TLR9-CTD structure (not shown). The significance of these, if any, remains unclear, although it is tempting to suggest some of these may be phosphate binding sites for DNA. An alignment of the TLR9-CTD with the TLR8-CTD and TLR3-CTD shows that the TLR9-CTD is more similar to TLR8-CTD (Fig. 2), with a Cα RMSD of 1.06Å for the TLR8 alignment (for 273 Cα) compared to 2.75Å for the alignment with TLR3. Also, the secondary structure elements in TLR9-CTD are noticeably more similar to those of TLR8-CTD.

One unique feature observed in the TLR9-CTD structure is the stacking of the side chains of four adjacent aromatic residues and one arginine, where the arginine is coplanar with the adjacent histidine and forms a pi-cation interaction (Fig. S1C). These residues are conserved amongst TLR9 sequences from various species, including mice (Fig. S2). While the stacking of these side chains likely plays a structural role, it is not clear yet whether or not there is also a functional role.

Based on several observations, we predict that the overall structure of the full-length TLR9 ectodomain is similar to that of TLR8, where the solenoid of LRRs forms a closed ring-like structure. First, the amino acid identity, number of LRRs, and location of extended loops suggest that the TLR9 structure should be more similar to TLR8 than to TLR3. Second, both the overall structure and the secondary structures of TLR9-CTD and TLR8-CTD match closely.

Predicting the ligand binding and activation mode for TLR9 is more challenging. Our best sources for drawing insight are the TLR8 and TLR3:dsRNA structures. However, as discussed above, TLR9 appears to be more closely related to TLR8 than to TLR3. Additionally, the details of ssRNA binding and activation of TLR8 remain unclear. No structure of TLR8 bound to a natural ligand is available with the only liganded structures of TLR8 being with small synthetic compounds. In fact, it is still unclear whether the natural ligands for TLR8 are ssRNA oligomers or single RNA nucleoside(s)[7].

We can, however, make a couple of reasonable predictions with the aid of some additional biochemical/biophysical evidence. First, it is likely that DNA is bound by TLR9 across the

entire length of the ascending lateral faces of the dimer similar to binding of dsRNA by TLR3. This notion is supported by two studies demonstrating that, in addition to the C-terminus, the N-terminus of TLR9 is essential for signaling[10,11]. Second, it is likely that TLR9 undergoes a conformational change upon ligand binding that is similar to that seen for TLR8, with each ectodomain rotating in opposite directions relative to one another. We show that TLR9 is similar to TLR8 structurally and in terms of LRR organization, and other studies show that TLR9 undergoes a conformational change upon DNA binding that brings the TIR domains into proximity[21]. The same may be true of the TLR9-CTD, as it is capable of binding DNA, can form dimers, and can activating downstream signaling[8].

Thus, we propose the following model for ligand binding and activation of TLR9. The full-length ectodomain, which forms a closed ring structure similar to TLR8, binds DNA in a manner similar to the TLR3:dsRNA interaction (Fig. S3, top). Both the N- and C-terminal domains interact with DNA, inducing a conformational change, bringing the two TIR domains into proximity, inducing signal transduction. For the CTD, DNA induces dimerization and the same conformational change, leading to activation (Fig. S3, bottom).

Conclusion

The crystal structure of the TLR9-CTD demonstrates its similarity to the TLR8-CTD. The TLR9-CTD exhibits the unique feature of extended aromatic side chain stacking on its the concave face. Thus, as TLR9 is structurally similar to TLR8, it presumably binds DNA in a manner similar to dsRNA binding by TLR3. However, structural studies will be required to elucidate its precise mode of interaction with DNA and mechanism of activation that would include studies of the full-length ectodomain and the CTD bound to DNA ligands.

Acknowledgements

We are grateful to P.S. Lee for help with X-ray data processing and useful discussions. We thank H. Tien at the Robotics Core of the Joint Center for Structural Genomics (JCSG) for automated crystal screening. X-ray data sets were collected at the Advanced Photon Source beamline 23-ID. Use of the APS was supported by the DOE, Basic Energy Sciences, Office of Science, under contract no. DE-AC02-06CH11357. This work is supported by NIH grants R01A1042266 (I.A.W.) and a Molecular Basis of Viral Pathogenesis training grant 5T32AI007354 (B.C.). This is publication number 27049 from The Scripps Research Institute.

Grant Sponsor: NIH grants R01 AI042266, Training Grant 5T32AI007354 (B.C.)

References

1. Kawai T, Akira S. Toll-like receptors and their crosstalk with other innate receptors in infection and immunity. Immunity. 2011; 34(5):637–650. [PubMed: 21616434]
2. Savva A, Roger T. Targeting Toll-Like Receptors: Promising Therapeutic Strategies for the Management of Sepsis-Associated Pathology and Infectious Diseases. Front Immunol. 2013; 4:2013.
3. Ewald SE, Barton GM. Nucleic acid sensing Toll-like receptors in autoimmunity. Curr Opin Immunol. 2011; 23(1):3–9. [PubMed: 21146971]
4. Brencicova E, Diebold SS. Nucleic acids and endosomal pattern recognition: how to tell friend from foe? Front Cell Infect Microbiol. 2013; 3:2013.
5. Botos I, Segal DM, Davies DR. The structural biology of Toll-like receptors. Structure. 2011; 19(4): 447–459. [PubMed: 21481769]

6. Leifer CA, Kennedy MN, Mazzoni A, Lee C, Kruhlak MJ, Segal DM. TLR9 is localized in the endoplasmic reticulum prior to stimulation. J Immunol. 2004; 173(2):1179–1183. [PubMed: 15240708]
7. Tanji H, Ohto U, Shibata T, Miyake K, Shimizu T. Structural reorganization of the Toll-like receptor 8 dimer induced by agonistic ligands. Science. 2013; 339(6126):1426–1429. [PubMed: 23520111]
8. Li Y, Berke IC, Modis Y. DNA binding to proteolytically activated TLR9 is sequence-independent and enhanced by DNA curvature. EMBO J. 2012; 31(4):919–931. [PubMed: 22258621]
9. Bauer S. Toll-like receptor 9 processing: the key event in Toll-like receptor 9 activation? Immunol Lett. 2013; 149(1-2):85–87. [PubMed: 23183093]
10. Onji M, Kanno A, Saitoh S, Fukui R, Motoi Y, Shibata T, Matsumoto F, Lamichhane A, Sato S, Kiyono H, Yamamoto K, Miyake K. An essential role for the N-terminal fragment of Toll-like receptor 9 in DNA sensing. Nat Commun. 2013; 4:2013. [PubMed: 23771051]
11. Peter ME, Kubarenko AV, Weber AN, Dalpke AH. Identification of an N-terminal recognition site in TLR9 that contributes to CpG-DNA-mediated receptor activation. J Immunol. 2009; 182(12): 7690–7697. [PubMed: 19494293]
12. Choe J, Kelker MS, Wilson IA. Crystal structure of human toll-like receptor 3 (TLR3) ectodomain. Science. 2005; 309(5734):581–585. [PubMed: 15961631]
13. Liu L, Botos I, Wang Y, Leonard JN, Shiloach J, Segal DM, Davies DR. Structural basis of toll-like receptor 3 signaling with double-stranded RNA. Science. 2008; 320(5874):379–381. [PubMed: 18420935]
14. Gosu V, Basith S, Kwon OP, Choi S. Therapeutic applications of nucleic acids and their analogues in Toll-like receptor signaling. Molecules. 2012; 17(11):13503–13529. [PubMed: 23151919]
15. Kabsch W. Xds. Acta Crystallogr D Biol Crystallogr. 2010; 66:125–132. Pt 2. [PubMed: 20124692]
16. Adams PD, Afonine PV, Bunkoczi G, Chen VB, Davis IW, Echols N, Headd JJ, Hung LW, Kapral GJ, Grosse-Kunstleve RW, McCoy AJ, Moriarty NW, Oeffner R, Read RJ, Richardson DC, Richardson JS, Terwilliger TC, Zwart PH. PHENIX: a comprehensive Python-based system for macromolecular structure solution. Acta Crystallogr D Biol Crystallogr. 2010; 66:213–221. Pt 2. [PubMed: 20124702]
17. Kim HM, Park BS, Kim JI, Kim SE, Lee J, Oh SC, Enkhbayar P, Matsushima N, Lee H, Yoo OJ, Lee JO. Crystal structure of the TLR4-MD-2 complex with bound endotoxin antagonist Eritoran. Cell. 2007; 130(5):906–917. [PubMed: 17803912]
18. Jin MS, Kim SE, Heo JY, Lee ME, Kim HM, Paik SG, Lee H, Lee JO. Crystal structure of the TLR1-TLR2 heterodimer induced by binding of a tri-acylated lipopeptide. Cell. 2007; 130(6): 1071–1082. [PubMed: 17889651]
19. Emsley P, Lohkamp B, Scott WG, Cowtan K. Features and development of Coot. Acta Crystallogr D Biol Crystallogr. 2010; 66:486–501. Pt 4. [PubMed: 20383002]
20. Jin MS, Lee JO. Application of hybrid LRR technique to protein crystallization. BMB Rep. 2008; 41(5):353–357. [PubMed: 18510864]
21. Latz E, Verma A, Visintin A, Gong M, Sirois CM, Klein DC, Monks BG, McKnight CJ, Lamphier MS, Duprex WP, Espevik T, Golenbock DT. Ligand-induced conformational changes allosterically activate Toll-like receptor 9. Nat Immunol. 2007; 8(7):772–779. [PubMed: 17572678]

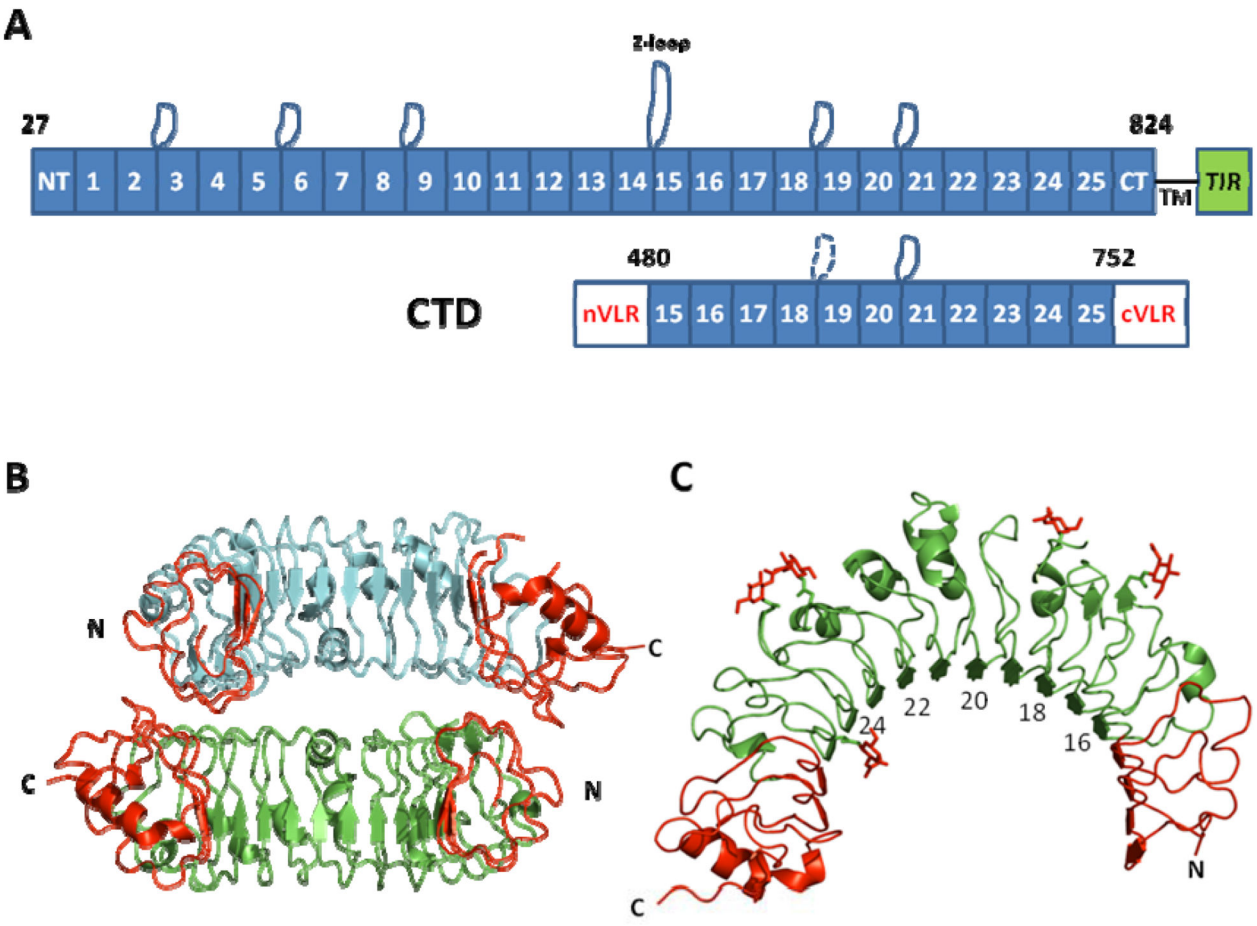

Fig. 1.

Structure of mTLR9-CTD. (A) Schematic representation of full-length TLR9 (excluding the signal sequence) (top) and TLR9-CTD (bottom). LRRs are indicated by numbered boxes. The long protruding loops between LRRs are indicated by curved lines above the LRRs (LRR18 loop lacked electron density for four residues and is represented by a dashed curved line). TM, transmembrane. (B) Cartoon representation of the TLR9-CTD non-crystallographic symmetry mates in the asymmetric unit. (VLR caps are colored in red.) (C) View of the ascending lateral face (probable ligand binding surface) of the TLR9-CTD monomer (N-glycans are colored in red and selected LRRs are numbered).

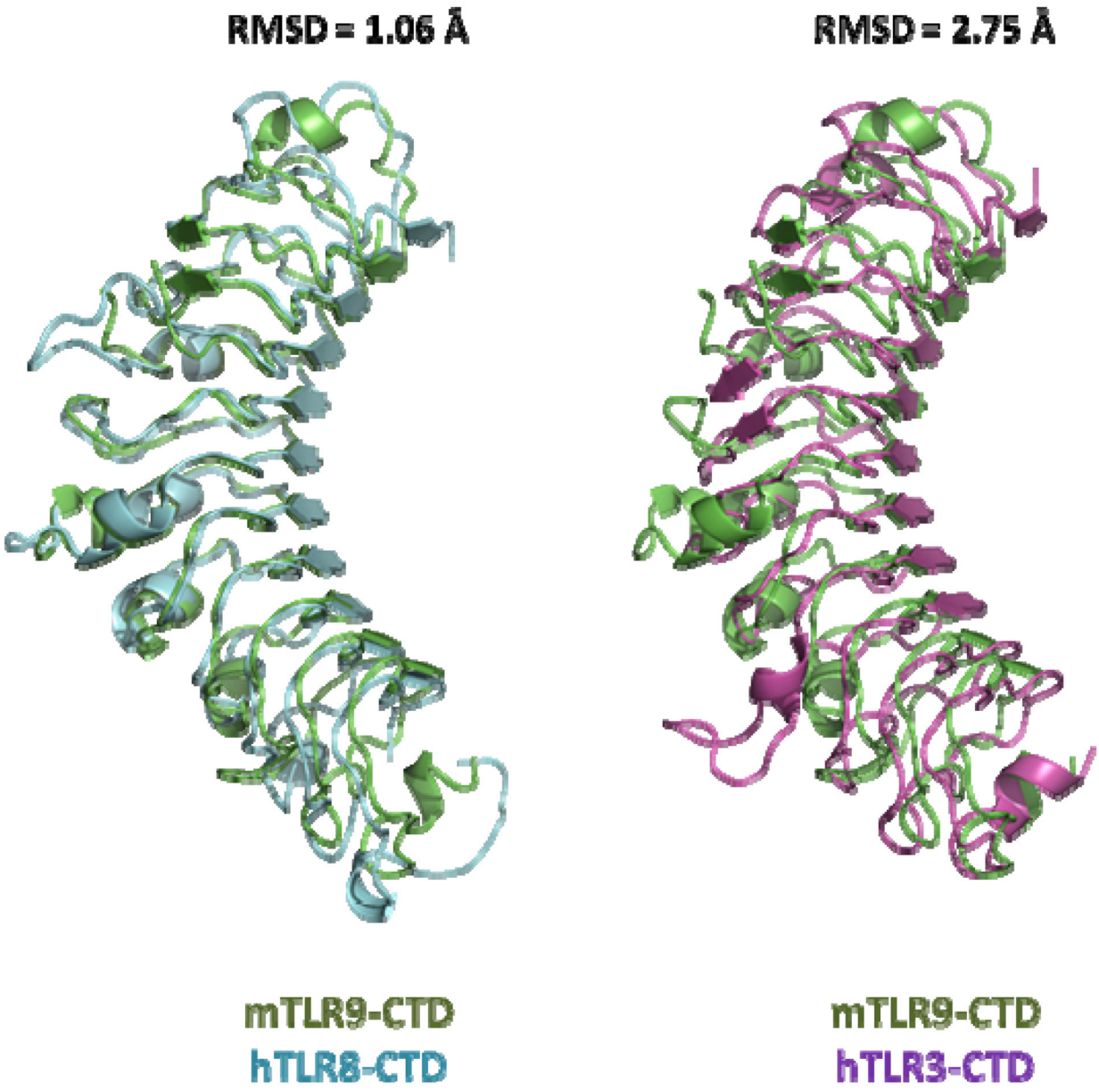

Fig. 2.

Comparison of the mTLR9-CTD structure with hTLR8 and hTLR3 counterparts. Alignment of mTLR9-CTD (green) with hTLR8-CTD (cyan) (PDBID 3W3G) (left) and hTLR3-CTD (magenta) (PDBID 2A0Z) (right). Alignment was performed using Pymol (www.pymol.org).

Table I

Data collection and refinement statistics

Data collection	
Beamline	APS 23ID
Wavelength (Å)	0.979390
Space group	$P3_121$
Unit cell parameters (Å,°)	a = b=106.03, c = 221.55,
Resolution (Å)	47.8-2.4 (2.47-2.40) [a]
Observations	210,475
Unique reflections	57,098 (4,388) [a]
Redundancy	3.7 (3.7) [a]
Completeness (%)	99.8 (99.4) [a]
$<I>/<\sigma_I>$	6.8 (1.7) [a]
R_{sym} [b]	0.13 (0.73) [a, b]
R_{pim} [c]	0.08 (0.44) [a, c]
Refinement statistics	
Resolution (Å)	47.8-2.4 (2.44-2.40)
Reflections (work)	57,039 (2,480)
Reflections (test)	2888 (119)
R_{cryst}(%)[d]	21.4 (29.3)
R_{free}(%)[e]	24.5 (32.3)
Average B-value (Å^2)	41
Wilson B-value (Å^2)	38
RMSD from ideal geometry	
Bond length (Å)	0.009
Bond angles (°)	1.50
Ramachandran statistics (%)[f]	
Favored	99.87
Outliers	0.13
PDB ID	

[a] Numbers in parentheses refer to the highest resolution shell.

[b] $R_{sym} = \Sigma_{hkl} \Sigma_i | I_{hkl,i} - <I_{hkl}> | / \Sigma_{hkl} \Sigma_i I_{hkl,I}$, where $I_{hkl,i}$ is the scaled intensity of the i^{th} measurement of reflection h, k, l, $< I_{hkl} >$ is the average intensity for that reflection, and n is the redundancy.

[c] R_{pim} is a redundancy-independent measure of the quality of intensity measurements. $R_{pim} = \Sigma_{hkl} (1/(n-1))^{1/2} \Sigma_i | I_{hkl,i} - \langle I_{hkl} \rangle | / \Sigma_{hkl} \Sigma_i I_{hkl,I}$, where $I_{hkl,i}$ is the scaled intensity of the i^{th} measurement of reflection h, k, l, $\langle I_{hkl} \rangle$ is the average intensity for that reflection, and n is the redundancy.

[d] $R_{cryst} = \Sigma_{hkl} | F_o - F_c | / \Sigma_{hkl} | F_o | \times 100$

[e] R_{free} was calculated as for R_{cryst}, but on a test set comprising 5% of the data excluded from refinement.

[f] These values were calculated using MolProbity (http://molprobity.biochem.duke.edu/).